Magnetoresistance in Double Spin Filter Tunnel Junctions with Nonmagnetic Electrodes and its Unconventional Bias Dependence

Guo-Xing Miao,* Martina Müller, and Jagadeesh S. Moodera

Francis Bitter Magnet Lab, Massachusetts Institute of Technology, Cambridge, Massachusetts 02139, USA

(Received 18 October 2008; published 17 February 2009)

Spin filtering happens due to the discriminative tunneling probabilities for spin-up and spin-down electrons through a magnetic barrier and can result in highly spin polarized tunnel currents. Combining two such barriers in a tunnel junction thus leads to large magnetoresistance without the necessity of magnetic electrodes. We demonstrate the realization of such unconventional tunnel junctions using double EuS spin filter barriers with Al electrodes. The novel nonmonotonic and asymmetric bias behavior in magnetoresistance can be qualitatively modeled in the framework of WKB approximations.

DOI: 10.1103/PhysRevLett.102.076601 PACS numbers: 72.25.−b, 73.43.Qt, 75.50.Pp

Magnetic tunnel junctions (MTJ) are of tremendous technological importance and widely applied in modern spintronic devices [1]. Since the first successful demonstration of room temperature (RT) tunnel magnetoresistance (TMR) [2], the maximum achieved TMR ratio has experienced a steady increase and recently reached over 500% at RT [3]. There have been various approaches to realize large TMR ratios. In the early generations of MTJs, amorphous tunnel barriers were utilized, and TMR is mostly determined by the spin density of states (DOS) of the two ferromagnetic (FM) electrodes involved and well described in Julliere's model [4]. A lot of effort has been devoted to constructing highly spin polarized metals (such as half-metals) to serve as the electrodes. Julliere's simple model has encountered difficulties when epitaxial tunnel barriers are utilized. It was found later on that, when the electron's Bloch state symmetry is also conserved in the tunneling process (termed the coherent tunneling), even conventional transition metal FM electrodes with ~40% spin polarization at the Fermi level can generate nearly completely spin polarized tunnel current through a symmetry filtering process, leading to giant TMR and effective spin injection [5,6]. Such symmetry filtering is established in certain crystallized tunnel barriers (textured or epitaxial) which preferentially allow electrons with matching Bloch state symmetry to pass more efficiently. Spin filtering (SF), on the other hand, takes an alternative approach [7]: using the unique property of a magnetic tunnel barrier to differentiate electrons' spins directly, rather than their symmetry. Starting with an unpolarized metallic electrode, spin-up and spin-down electrons passing a SF tunnel barrier are selectively filtered through the tailoring of tunneling probabilities, due to the different tunnel barrier heights for the two spin channels. As a consequence, highly spin polarized current can be generated from a completely unpolarized source electrode [8]. Large magnetoresistance (MR) has been predicted in double SF tunnel junctions [9–11]. In the proposed NM/SF/SF/NM [9,10] and NM/SF/NM/SF/NM [11] types of junctions, both electrodes are unpolarized normal metals (NM), and the MR originates from the spin selective barrier heights when the two SF barriers are toggled between parallel (P) and antiparallel (AP) states. Experimentally, however, only quasi-SF tunnel junctions have been realized to date [12–16], in which a conventional FM counter-electrode still serves as the spin detector. In this letter, we show the first successful demonstration of MR in a double SF barrier tunnel junction, with no FM electrodes involved, purely by tuning the tunneling probabilities. Moreover, we observe a highly unconventional MR bias dependence in these junctions. By applying a numerical model based on Wentzel-Kramers-Brillouin (WKB) approximation, we can qualitatively explain the origin of the pronounced MR peaks in both bias polarities, as well as the dramatic bias and magnitude asymmetry seen in these junctions.

We fabricated the SF tunnel junction structures by thermal evaporation using *in situ* shadow masks, in a vacuum system with base pressure of 7×10^{-8} torr. The whole stack was deposited on glass substrates, with 10 nm thick Al cross bars as the top and bottom electrodes. The effective junction area was $200 \times 200\ \mu m^2$. The tunnel barrier consisted of two EuS layers magnetically decoupled by a 0.6 nm thick Al_2O_3 layer, with all barrier layers *e*-beam evaporated. In order to separate the coercive fields of the two EuS layers, the bottom EuS layer was deposited at liquid nitrogen (LN) temperature, whereas the top EuS layer was deposited at RT. SQUID measurement confirmed that these two types of EuS films have different magnetic switching characteristics: LN deposited EuS films are magnetically softer with much sharper hysteretic switching compared to RT deposited films. This difference can be attributed to the variation in the film growth modes, while T_C was not much different between these two types of films. Details on EuS film properties will be described elsewhere. The tunnel junctions were fully submerged in a pumped liquid He^4 bath, at 1 K, during the transport measurement.

When EuS undergoes the paramagnetic-ferromagnetic transition, the ferromagnetic ordering of the Eu $4f^7$ states causes the conduction band to split into two energy levels,

with the up-spin energy levels lowered by Δ_{ex} while the down-spin energy levels raised by Δ_{ex}. When it is used as a tunnel barrier, the spin-up and spin-down electrons experience different tunnel barrier heights and their corresponding tunneling probabilities can easily differ by orders of magnitude, due to the exponential dependence on barrier heights. The principle of double SF tunnel junction is illustrated in Fig. 1, top panel: in the P alignment the spin-up electrons experience a much lower average tunnel barrier height and thus lead to a low total junction resistance; while in the AP alignment electrons from both channels have to cross at least one high barrier in order to get through, and the junction resistance is higher.

In WKB approximations, the transmission probability T for an electron with energy E can be expressed as follows:

$$T_\sigma(E) \cong \exp\left[-2\int_0^d \sqrt{\frac{2m_e}{\hbar^2}(\varphi_\sigma(x) - E)}dx\right]. \quad (1)$$

Here m_e is the free electron mass, and φ_σ is the barrier height for each spin channel $\sigma = \uparrow, \downarrow$ at position x within the barrier region which extends from 0 to d. Since the tunneling electrons' wave vectors can become real in certain regions of the barrier Fowler-Nordheim (FN) tunneling [17] occurs, and such plane waves do not contribute to the tunneling probability decay, our calculation of $T_\sigma(E)$ is only performed in regions where quantum tunneling happens (i.e., where $E < \varphi_\sigma(x)$) and neglects any interferences or scattering events. To account for the total dc conductance under finite biases, we performed integration over all the available states when the Fermi level of one electrode is raised above that of the other (schematic shown in Fig. 1, bottom panel inset). Mathematically, the total dc conductance G at bias voltage V is expressed as follows,

$$G \propto \sum_\sigma \int_{-\infty}^{\infty} N_{1\sigma}(E)N_{2\sigma}(E + eV)T_\sigma(E) \times [f(E) - f(E + eV)]dE. \quad (2)$$

Here $f(E)$ is the Fermi distribution function and $N_{1\sigma}$, $N_{2\sigma}$ are the DOS of the electrodes on the two sides. The summation over σ ensures the consideration of the conductance from both spin channels. For simplicity, we have assumed that the Al electrodes have flat DOS throughout the voltage range we are exploring, and that the electric field is distributed homogeneously across the barrier. Because of the large barrier thickness involved, only electrons incident normal to the barrier (i.e., $k_\parallel = 0$) were taken into account in this calculation. The MR ratio is now simply $\mathrm{MR} = (G_P - G_{AP})/G_{AP}$. We applied the above formula to a realistic system based on $EuS/Al_2O_3/EuS$ hybrid tunnel barriers. EuS orders ferromagnetically with a bulk Curie temperature (T_C) of 16.6 K [18]. The reported tunnel barrier height φ_0 and the exchange splitting $2\Delta_{ex}$ are 0.8 and 0.36 eV, respectively [18,19]. For the film thicknesses ($\sim$3 nm) used in our experiments, T_C is around 11 K according to SQUID measurements. This suggests that the average exchange splitting in thin films is smaller than the bulk value. We adopt a value of $2\Delta_{ex} \sim 0.24$ eV in our calculations, based on the assumption that T_C is proportional to Δ_{ex} [20] and neglecting the variations of T_C in the thickness range we are studying. A barrier height value of 1 eV is assumed for the ultrathin Al_2O_3 spacer layer in the modeling. We performed most measurement at 1 K, $\ll T_C$. Thus in our calculation we evaluated the conductance at 0 K only, and the integral in Eq. (2) is significantly simplified and becomes a finite integral of $T_\sigma(E)$ from $-$eV to 0 (as illustrated in Fig. 1, bottom panel inset). For each bias voltage V, the double integral was calculated by numerically summing over a mesh with even spacing of 0.001 nm in thickness and $V/1000$ in voltage, respectively.

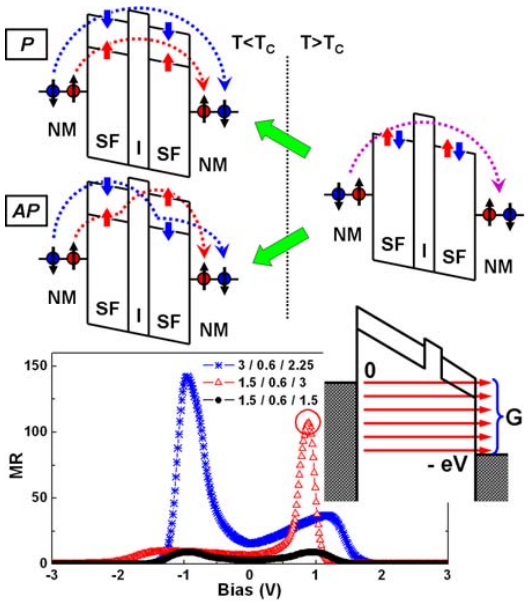

FIG. 1 (color online). (Top panel) schematic illustration of the SF mechanism in double SF tunnel junctions across T_C. Dotted lines roughly indicate the barriers that the spin-up and spin-down electrons have to cross. (Bottom panel) calculated MR bias dependence. The label indicates the $EuS/Al_2O_3/EuS$ barrier layers' thicknesses (in nm) from bottom to top. The inset is a schematic illustration of the calculation method: the dc conductance is an integration of the tunnel probabilities from all the available states for a given applied bias [Eq. (2)]. It also approximately shows the Fermi level alignment for the peak MR which is circled out on the calculated bias curve [21].

The result of the calculated MR ratio is plotted in Fig. 1, bottom panel. In these double SF tunnel junctions, the first SF barrier functions as the spin polarizer that generates a highly polarized current, whereas the second SF barrier serves as the spin analyzer whose P and AP magnetic alignment relative to the first SF layer leads to the large conductance differences. Increasing the SF barrier thickness will largely enhance MR, as can be seen from the systematic increase of the zero bias MR in Fig. 1. When the applied voltage exceeds the spin-up barrier height ($\varphi_0 - \Delta_{ex}$), the FN tunneling occurs and increases MR dramati-

cally [10,15], leading to very pronounced MR peaks in both bias voltage polarities. When the Fermi level of the source electrode approximately matches the averaged spin-up barrier height on the analyzer side (Fig. 1, inset) [21], the spin-up electrons possess strongly enhanced tunneling probability due to FN tunneling, while the spin-down electrons only show limited or no FN tunneling. This leads to the maximum difference in the tunneling probability for spin-up and spin-down electrons and hence the maximum MR. Further increase in bias voltage will allow significant FN tunneling of the spin-down electrons, and reduces MR instead.

Different thickness of the two SF barriers is thus responsible for the asymmetric position and magnitude of MR peaks as seen in Fig. 1. When electrons are going from a thicker SF into a thinner SF, less bias voltage is required to establish maximum difference in the FN tunneling. It is also beneficial to use a thick spin polarizer layer coupled with a thin spin analyzer layer in order to achieve a large MR, as can be clearly seen from the asymmetry in the MR peak heights. This is because the spin polarizing power of the first SF layer is exponentially dependent on its thickness, which generates the highly polarized current that dominates the tunneling process. Thus the SF layer thickness and the applied bias polarity allows for the choice of MR peak position as well as its intensity. It is worth pointing out here that the zero bias MR values in our calculation match the previous calculation [9] very closely, and our inclusion of Al_2O_3 spacer layer does not influence the zero bias MR. On the other hand, when higher bias is considered, introducing Al_2O_3 spacer layer reduces the maximum MR and shifts the peaks towards lower voltages.

Experimentally, we indeed observed the dramatic asymmetry in the MR bias dependence as predicted from our above numerical calculations. We deduce the MR bias dependence from the IV curves taken in the P and AP configurations. In the low bias regime, below the onset of FN tunneling, the junction resistance is well above 10^9 Ω and as such we could not obtain reliable experimental results to compare with theory. For thicker junctions, the bias voltage could be increased up to 3 V before the junctions suffered irreversible resistance change or complete breakdown. The breakdown electric field was on the order of 10^9 V/m. Figure 2 shows the MR loop and bias dependence in a double SF tunnel junction (layers from bottom to top, in nm): 10 Al/1.5 EuS/0.6 Al_2O_3/3 EuS/10 Al. The top EuS layer is thicker than the bottom layer, yielding higher MR in the positive bias regime when the electrons are traveling from top to bottom. A noticeable resistance decrease was observed when the sample was cooled below the T_C of EuS, as a signature of the SF effect [Fig. 2(c)] [22], and further decrease can be seen between 4.2 and 1 K [Fig. 2(b)]. The MR increase at low temperature can be mainly due to a more pronounced coercivity separation between the two EuS layers, as well as the likely suppression of both spin flipping and thermal assisted tunneling. Figure 3(a) shows the MR bias dependence of several junctions with the SF layer thickness chosen to match the calculation as shown in Fig. 1. We observe that the theoretical modeling is in good qualitative agreement with the experimental results. Figure 3(b) shows the junction MR and resistance asymmetry with one SF layer thickness being fixed, while varying the thickness of the other SF layer. We define the ''magnitude asymmetry'' in MR and resistance as their relative changes between +1.2 V and −1.2 V bias. The bias strength is fixed to allow for direct comparison of the junction resistances that vary strongly with applied voltage, while the value 1.2 V is chosen such that the TMR values obtained are still very close to the peak values in these samples. Clearly the magnitude asymmetry shows opposite trends for MR and resistance: larger MR is accompanied by lower resistance, due to the presence of stronger FN tunneling. Such asymmetry vanishes roughly when the thicknesses of the two SF layers are equal.

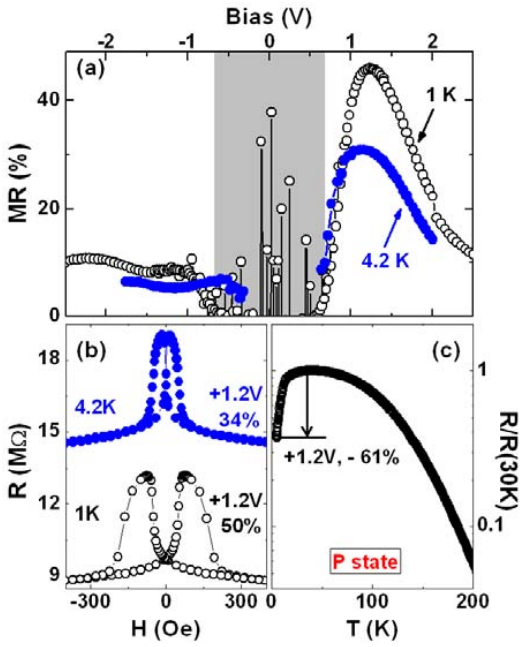

FIG. 2 (color online). MR in a SF tunnel junction with (in nm): 10 Al/1.5 EuS/0.6 Al_2O_3/3 EuS/10 Al. (a) Bias dependence at 4.2 K (closed circles) and 1 K (open circles). Shaded part indicates the regions below the onset of FN tunneling and is much noisier due to the extremely high impedance. (b) MR loop at 4.2 K (closed circles) and 1 K (open circles) with +1.2 V bias voltages. (c) Normalized junction resistance as a function of temperature, measured in P state under +1.2 V bias voltage.

Although the model calculation matches our experimental results qualitatively, there is insufficient quantitative agreement. We note here that no adjustable parameters have been introduced in our numerical calculation, all values have been taken from the literature or determined in experiment. The treatment of the barriers as of rigid trapezoidal shapes is not completely plausible: the formation of image forces in the electrodes, and the weakening of exchange splitting on SF layer surfaces, both have the effect

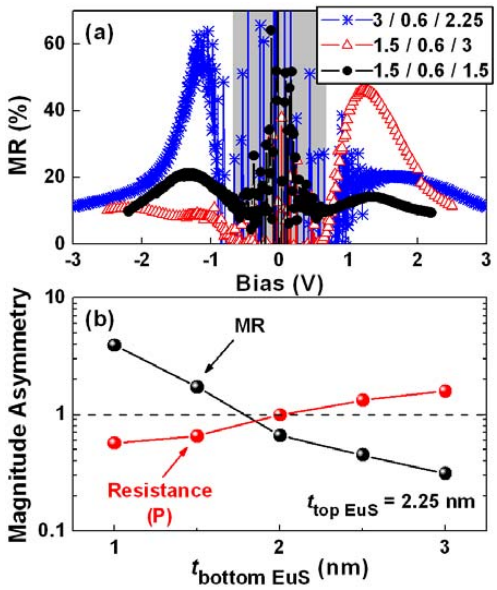

FIG. 3 (color online). (a) Measured bias dependence for the SF tunnel junctions. The label indicates the $EuS/Al_2O_3/EuS$ barrier layers' thicknesses (in nm) from bottom to top. Shaded part indicates the regions below the onset of FN tunneling and is much noisier due to the extremely high impedance. (b) The magnitude asymmetry in resistance and MR between ± 1.2 V. The top EuS layer and the spacer Al_2O_3 layer thickness are fixed at 2.25 and 0.6 nm, respectively.

of distorting the barriers away from simple trapezoidal shapes. The largest discrepancy between theory and experiment can be found in the difference of the maximum MR values. We observed up to 60% MR, while the theoretical predictions (in an ideal case) are 2 orders of magnitude higher. Choosing a significantly smaller exchange splitting $2\Delta_{ex}$ can lead to comparable results. However, in the thin films we are studying, the measured T_C is around 11 K, meaning that the exchange splitting cannot be too low (a value of 0.04 eV with a $T_C < 2$ K is needed to match the MR number). Instead, several other factors can account for the reduction of the actual MR. The nonperfect interfaces in the real samples could reduce MR significantly. At the tunnel barrier thicknesses we were dealing with, tunneling electrons can cross the barrier by multistep hopping via trap states, which is not accounted for in our model. With the excess energy involved at high biases, the tunneling electrons can excite various elemental excitations (such as photons, phonons, and magnons) within the barrier, and easily lose their spin orientation, momentum and energy. These processes can reduce the spin filtering efficiency and suppress TMR dramatically. The presence of inelastic tunneling processes also significantly broadens the MR peaks and shifts them towards higher voltages. We would like to point out here that the large tunnel barrier thickness (consisting of triple barriers) and the resultant suppression to single step tunneling, would probably be a universal limiting factor in such SF tunnel junctions for achieving higher TMR.

In summary, we have demonstrated the successful realization of double SF tunnel junctions based on nonmagnetic Al electrodes and EuS SF barriers. The observed MR showed pronounced peaks and significant asymmetry in the bias dependence. We used a simple model based on WKB approximation to numerically calculate the MR bias dependence, and the result showed qualitative agreement with the experiment. The modeling reveals the origin of such asymmetric behavior.

This work is supported by NSF and ONR research grants. M. M. thanks the German Academic Exchange Service (DAAD) for financial support.

*gxmiao@mit.edu

[1] I. Zutic, J. Fabian, and S. D. Sarma, Rev. Mod. Phys. **76**, 323 (2004).
[2] J. S. Moodera, L. R. Kinder, T. M. Wong, and R. Meservey, Phys. Rev. Lett. **74**, 3273 (1995).
[3] Y. M. Lee *et al.*, Appl. Phys. Lett. **90**, 212507 (2007).
[4] M. Julliere, Phys. Lett. A **54**, 225 (1975).
[5] W. H. Butler, X.-G. Zhang, T. C. Schulthess, and J. M. MacLaren, Phys. Rev. B **63**, 054416 (2001).
[6] J. Mathon and A. Umerski, Phys. Rev. B **63**, 220403(R) (2001).
[7] J. S. Moodera, T. S. Santos, and T. Nagahama, J. Phys. Condens. Matter **19**, 165202 (2007).
[8] J. S. Moodera, X. Hao, G. A. Gibson, and R. T. Meservey, Phys. Rev. Lett. **61**, 637 (1988); T. S. Santos and J. S. Moodera, Phys. Rev. B **69**, 241203(R) (2004).
[9] D. C. Worledge and T. H. Geballe, J. Appl. Phys. **88**, 5277 (2000).
[10] Z. W. Xie and B. Z. Li, J. Appl. Phys. **93**, 9111 (2003).
[11] A. Saffarzadeh, J. Phys. Condens. Matter **15**, 3041 (2003).
[12] P. LeClair *et al.*, Appl. Phys. Lett. **80**, 625 (2002).
[13] U. Luders *et al.*, Appl. Phys. Lett. **88**, 082505 (2006); U. Luders *et al.*, Phys. Rev. B **76**, 134412 (2007).
[14] A. V. Ramos *et al.*, Appl. Phys. Lett. **91**, 122107 (2007).
[15] T. Nagahama, T. S. Santos, and J. S. Moodera, Phys. Rev. Lett. **99**, 016602 (2007).
[16] M. Gajek *et al.*, Phys. Rev. B **72**, 020406(R) (2005); M. Gajek *et al.*, Nature Mater. **6**, 296 (2007).
[17] R. H. Fowler and L. Nordheim, Proc. R. Soc. A **119**, 173 (1928).
[18] K. A. Gschneidner, Jr. and L. R. Eyring, *Handbook on the Physics and Chemistry of Rare Earths* (North-Holland, New York, 1979), Vol. 2.
[19] X. Hao, Ph.D. thesis, Massachusetts Institute of Technology, 1990.
[20] R. C. O'Handley, *Modern Magnetic Materials: Principles and Applications* (Wiley-Interscience, New York, 2000).
[21] According to our calculation, at peak MR the Fermi level is roughly aligned in the middle of the tilted spin-up barrier (indicates as a star in Fig. 1 inset), and its exact position depends on the assumed exchange splitting Δ_{ex}. It moves towards lower voltages for smaller Δ_{ex} and towards higher voltages for larger Δ_{ex}.
[22] T. S. Santos *et al.*, Phys. Rev. Lett. **101**, 147201 (2008).